Available online at www.sciencedirect.com
ScienceDirect
Applied Catalysis A: General 326 (2007) 17–27
APPLIED CATALYSIS A: GENERAL
www.elsevier.com/locate/apcata

Reduction behavior of iron oxides in hydrogen and carbon monoxide atmospheres

W.K. Jozwiak, E. Kaczmarek *, T.P. Maniecki, W. Ignaczak, W. Maniukiewicz

Institute of General and Ecological Chemistry, Technical University of Lodz, 90-924 Lodz, Zeromskiego 116, Poland

Received 13 October 2006; received in revised form 19 February 2007; accepted 20 March 2007
Available online 30 March 2007

Abstract

The reduction of various iron oxides in hydrogen and carbon monoxide atmospheres has been investigated by temperature programmed reduction (TPR_{H2} and TPR_{CO}), thermo-gravimetric and differential temperature analysis (TG-DTA-MS), and conventional and "*in situ*" XRD methods. Five different compounds of iron oxides were characterized: hematite α-Fe_2O_3, goethite α-FeOOH, ferrihydrite $Fe_5HO_8{\cdot}4H_2O$, magnetite Fe_3O_4 and wüstite FeO. In the case of iron oxide-hydroxides, goethite and ferrihydrite, the reduction process takes place after accompanying dehydration below 300 °C. Instead of the commonly accepted two-stage reduction of hematite, 3 α-$Fe_2O_3 \rightarrow 2\ Fe_3O_4 \rightarrow 6$ Fe, three-stage mechanism $3Fe_2O_3 \rightarrow 2Fe_3O_4 \rightarrow 6FeO \rightarrow 6Fe$ is postulated especially when temperature of reduction overlaps 570 °C. Up to this temperature the postulated mechanism may also involve disproportionation reaction, $3Fe^{2+} \rightleftharpoons 2Fe^{3+} + Fe$, occurring at both the atomic scale on two-dimensional interface border Fe_3O_4/Fe or stoichiometrically equivalent and thermally induced, above 250 °C, phase transformation—wüstite disproportionation to magnetite and metallic iron, $4FeO \rightleftharpoons Fe_3O_4 + Fe$. Above 570 °C, the appearance of wüstite phase, as an intermediate of hematite reduction in hydrogen, was experimentally confirmed by "*in situ*" XRD method. In the case of FeO–H_2 system, instead of one-step simple reduction FeO → Fe, a much more complex two-step pathway FeO → Fe_3O_4 → Fe up to 570 °C or even the entire sequence of three-step process FeO → Fe_3O_4 → FeO → Fe up to 880 °C should be reconsidered as a result of the accompanying FeO disproportionation wüstite ⇌ magnetite + iron manifesting its role above 150 °C and occurring independently on the kind of atmosphere—inert argon or reductive hydrogen or carbon monoxide. The disproportionation reaction of FeO does not consume hydrogen and occurs above 200 °C much easier than FeO reduction in hydrogen above 350 °C. The main reason seems to result from different mechanistic pathways of disproportionation and reduction reactions. The disproportionation reaction wustite ⇌ magnetite + iron makes simple wüstite reduction FeO → Fe a much more complicated process. In the case of thermodynamically forced FeO disproportionation, the oxygen sub-lattice, a closely packed cubic network, does not change during wüstite → magnetite transformation, but the formation of metallic iron phase requires temperature activated diffusion of iron atoms into the region of inter-phase FeO/Fe_3O_4. Depending on TPR_{H2} conditions (heating rate, velocity and hydrogen concentration), the complete reduction of hematite into metallic iron phase can be accomplished at a relatively low temperature, below 380 °C. Although the reduction behavior is analogical for all examined iron oxides, it is strongly influenced by their size, crystallinity and the conditions of reduction.

Keywords: Iron oxide; Reduction process

1. Introduction

Many oxidic iron compounds—iron oxides, oxide-hydroxides and hydroxides—not only play an important role in a variety of disciplines and also serve as a model system of reduction and catalytic reactions [1]. Hematite α-Fe_2O_3 being a major and thermodynamically most stable oxide among the 16 identified iron oxidic compounds it is commonly used as an adsorbent, a catalyst precursor and an active component of catalytic material [1–6]. The CO reduction process of hematitic ores in blast furnace produces metallic iron *via* a series of intermediate oxides i.e. hematite α-Fe_2O_3 → magnetite Fe_3O_4 → wüstite FeO → iron Fe^0. The reduction of unsupported iron oxides and supported and/or promoted iron catalysts in hydrogen and/or carbon monoxide atmosphere has been studied extensively and plays an important role in many catalytic reactions: ammonia and Fisher-Tropsch synthesis, carbon monoxide hydrogenation, dehydrogenation of ethylbenzene to

* Corresponding author.
E-mail address: wjozwiak@p.lodz.pl (E. Kaczmarek).

0926-860X/$ – see front matter © 2007 Elsevier B.V. All rights reserved.
doi:10.1016/j.apcata.2007.03.021

styrene, NO_x and soot removal from diesel exhaust, water gas shift reaction and carbon monoxide oxidation [1–5]. A considerable attention has been devoted to certain well-established features of the transformation of hematite to magnetite, but despite extensive research efforts, the entire mechanism of the hematite reduction in hydrogen is still not fully understood [5–41]. The nature of the total process is extremely complex and may vary with the physicochemical characteristics of the iron oxide or with the conditions of its reduction [5]. The literature data diverge considerably since different iron oxides and oxy-hydroxides exist (α-Fe_2O_3, Fe_3O_4, FeO, α-$FeOOH{\cdot}xH_2O$, $Fe_5HO_8{\cdot}4H_2O$), and there are large differences in their reduction process, for instance, temperature range, water partial pressure, particle size and presence of additives or impurities. Iron oxides: Fe_2O_3, Fe_3O_4, FeO not only differ in their fundamental oxidation state but are also usually regarded as non-stoichrometric compounds reflecting their natural tendency for oxidation $Fe^{2+} \rightarrow Fe^{3+}$ (or hydration) and thee appropriate formulas are given in Table 1. The pathway of hematite reduction can be essentially different. The three-step mechanism $3Fe_2O_3 \rightarrow 2Fe_3O_4 \rightarrow 6FeO \rightarrow 6Fe$ is often postulated [4–13] instead of the commonly accepted two-step reduction $3Fe_2O_3 \rightarrow 2Fe_3O_4 \rightarrow 6Fe$ [13–16]. The entirely different pathway of hematite reduction $3Fe_2O_3 \rightarrow 6FeO \rightarrow 6Fe$ was also proposed [17]. In addition, wüstite was accepted as a final product of Fe_2O_3 reduction in hydrogen at a temperature range 300–400 °C [18]. Metastable FeO can be stabilized on the support surface or into iron phase with doping agents [19,20]. Taking into account the experimental differences, the quantitative and qualitative comparison of TPR profiles for hematite often leads to the unacceptably different conclusions. For example, the approval of two-step reduction $FeO_{1.5} \rightarrow FeO_{1.33} \rightarrow Fe$ cannot be favored by TPR_{H2} profiles in which unacceptable amounts of hydrogen are consumed in both reduction steps [21]. Although there are few mechanistic models of hematite reduction in hydrogen and carbon monoxide, common, the lack of certain details referring to the full experimental conformation still remains obvious. Also, there are only sparse and limited literature data referring to the reduction of different kinds of iron oxides, oxide-hydroxides and hydroxides.

This work focusses upon the temperature programmed reduction behavior of five different iron oxidic compounds: hematite α-Fe_2O_3, goethite α-FeOOH, ferrihydrite $Fe_5HO_8{\cdot}4H_2O$, magnetite Fe_3O_4 and wüstite FeO in hydrogen and carbon monoxide atmosphere. Although, the above compounds differ in the kind and nature of crystal phase, the presence of hydroxyl groups inside crystal network or on its surface and different oxidation state of iron atoms, one can anticipate rather general mechanistic properties related to the entire reduction process or its fractional reduction stages.

2. Experimental

2.1. Materials

Iron(III) oxide α-Fe_2O_3 (hematite) and iron(III) oxy-hydroxides α-$FeOOH{\cdot}xH_2O$ (goethite) and $Fe_5HO_8{\cdot}4H_2O$ (2-line ferrihydrite) were prepared from $Fe(NO_3)_3{\cdot}9H_2O$ and NH_3 aqueous solutions by precipitation method and drying at 60 °C [22]. In order to obtain hematite, the calcination of iron oxide-hydroxide precursor was done for 3 h at 600 °C in air. Iron oxide(II) FeO (wüstite) and iron oxide(II, III) Fe_3O_4 (magnetite) used as reference materials were purchased from Aldrich company.

2.2. Methods

The surface area measurements were carried out using BET (liquid N_2) method. The reduction studies were carried out using: TPR (AMI-1), TG-DTA-MS (Setsys 16/18) and conventional and "*in situ*" XRD methods.

Temperature programmed reduction (TPR_{H2} and TPR_{CO}) measurements were carried out in AMI-1 Altamira instrument. Prior to the TPR measurements, catalyst samples (usually 10 or 50 mg) were dried at 60 °C and/or calcined for 2 h at 200, 400 and 600 °C, respectively, in air or 10% O_2–90% Ar gas stream. The iron oxide samples were reduced in 5% H_2–95% Ar or 5% CO–95% Ar gas mixture with a volume flow rate of 50 $cm^3\ min^{-1}$ and a linear heating rate in the range from O.5 to 25 °C/min. TPR_{H2} profiles were recorded using thermo-conductive detector whereas TPR_{CO} profiles were recorded with mass spectrometer as a detector. The selected conditions of experiments were chosen to distinguish between mass transfer diffusion and kinetic effects of reduction [12,23,24].

Thermo-gravimetric (TG) method equipped with a differential thermal analysis (DTA) device SETSYS-16/18 (Setaram) and a mass spectrometer (MS, Balzers) was used for temperature programmed reduction of iron oxides in different reductive atmospheres: pure hydrogen (99.99% H_2) and 5% H_2–95% Ar or 5% CO–95% Ar gaseous mixtures. The TG–DTA–MS measurements were carried out applying a sample of weight about 10 mg with a linear growth of temperature, usually 1 or 10 °C per min, and temperature range from 25 to 1000 °C.

The conventional *XRD measurements* were carried out on Siemens D5000 powder X-ray diffractometer. It was operating with a scanning speed of 0.03° per 10 s. Diffractions patterns

Table 1
Non-stoichiometrical ferric oxides

Mineral	Stoichiometrical formula	Non-stoichiometrical formula
Hematite	α-Fe_2O_3	$Fe_{2-x/3}(OH)_xO_{3-x}$
Magnetite	Fe_3O_4	$Fe^{II}{}_{1-x}Fe^{III}{}_{2+x}O_{4+x/2}$ $(0 < x \geq 1)$
Wüstite	FeO	$Fe_{1-x}O$ $(0.83 < 1 - x < 0.95)$ $p = 0.1$ MPa, $T > 567$ °C

were recorded in the range $2\theta = 10–90^\circ$, using nickel-filtered Cu Kα radiation.

In "*in situ*" *XRD method* approximately 200 mg of iron oxide, which had been ground in an agate mortar, was packed in the glass ceramic (Macor) sample holder. Although the reagent gas mixture 5% H_2–95% Ar was used in the experiment to allow the complete reduction of iron oxide to metallic iron, yet it attenuates the reaction rate enough to allow the collection of an X-ray diffraction pattern at regular intervals. The sample was heated at a nominal rate of 1 °C per min. At every 20 °C X-ray diffraction data were collected using a PANalytical X'Pert Pro diffractometer equipped with an Anton Paar XRK900 reactor chamber. The electrical heater of the reactor chamber is designed to heat the volume of the sample with a minimal temperature gradient. The X-ray source was a long fine focus X-ray diffraction copper tube operating at 40 kV and 30 mA. Divergent optics were used in a Bragg–Brentano (flat-plate sample) geometry, with fixed divergence (1/2°) and antiscatter (1°) slits. Incident and receiving 0.04 rad Soller slits were used to limit axial divergence, and a curved graphite monochromator on the receiving side was used to eliminate Cu Kβ radiation. The sample was scanned at 3° per min in the range of 2θ from 28° to 70°. A PANalytical X'Celerator detector based on Real Time Multiple Strip technology capable of simultaneously measuring the intensities in the 2θ range of 2.122° was used. The analogical procedure was applied during the measurements of temperature activated X-ray phase composition changes in wüstite disproportionation reaction taking place in inert atmosphere of argon.

2.3. Quantitative phase analysis

Quantitative phase abundances were determined for hematite, magnetite, wüstite and iron using the High Score Plus package. In quantitative phase analysis using Rietveld method, the weight fraction W_i of each ith crystalline component in the mixture was calculated from the corresponding refined scale parameter S_i, according to the equation:

$$W = \frac{S_i M_i V_i}{\sum S_j M_j V_j},$$

where M_i and V_i are the unit cell mass and volume of ith crystalline component, respectively [25,26].

3. Results

3.1. Hydrogen reduction

The influence of the heating rate, in the range from 0.58 to 10.7 °C per min on TPR_{H2} profiles of hematite is presented in Fig. 1A and B for two sample masses about 50 and 15 mg, respectively.

Using the same volume flow rate of 5% H_2–95% Ar gas mixture (50 cm^3 min^{-1}), the temperature range of the entire reduction of hematite to metallic iron, Fe(III) → Fe(0), and the changes of TPR profile shape strongly depend on the heating rate. In order to accomplish this process in a low temperature range, up to about 450–480 °C, a slow heating rate of 0.58 °C per min is required, whereas with a relatively fast heating rate of 10.7 °C per min the complete reduction moves to much higher temperatures, up to about 700–800 °C. In less favorable conditions even much higher temperature up to 1250 °C was necessary to accomplish reduction of hematite [27]. The typical TPR_{H2} profile consists of two fairly well separated reduction peaks, the smaller low temperature peak taking up about 13% of total surface area under TPR curve, reflects the first stage of the reduction of hematite to magnetite α-$Fe_2O_3 \rightarrow Fe_3O_4$ and the second, broad and much larger, high temperature peak represents the reduction of magnetite to metallic iron $Fe_3O_4 \rightarrow \alpha$-Fe. In fact, in this high temperature region two heavily overlapped peaks can be observed, especially when higher heating rates of 5.52 and 10.7 °C per min are applied. These two TPR peaks are tentatively assigned to the two-step magnetite reduction sequence, 2 $Fe_3O_4 \rightarrow 6$ FeO → 6 Fe. The existence of wüstite phase as an intermediate of magnetite reduction was experimentally confirmed by the conventional XRD method when TPR_{H2} run was interrupted, in temperature range above 570 °C and sample was quickly cooled down in reducing stream (see XRD pattern 6 in Fig. 6). The prolonged contact of reduced hematite sample with hydrogen, accompanying TPR_{H2} run with low heating rate leads to considerable shift of both TPR peak maxima T_{max1} and T_{max2} toward lower temperatures, about 120 and 200 °C representing the reduction steps Fe_2O_3 to Fe_3O_4 and Fe_3O_4 to Fe, respectively (see broken lines in Fig. 1). The value of maximum temperature T_{max} is probably conditioned by a low temperature side of TPR peak representing self-catalyzed nucleation as a rate-determining step [14]. The first symptoms of hematite reduction may be

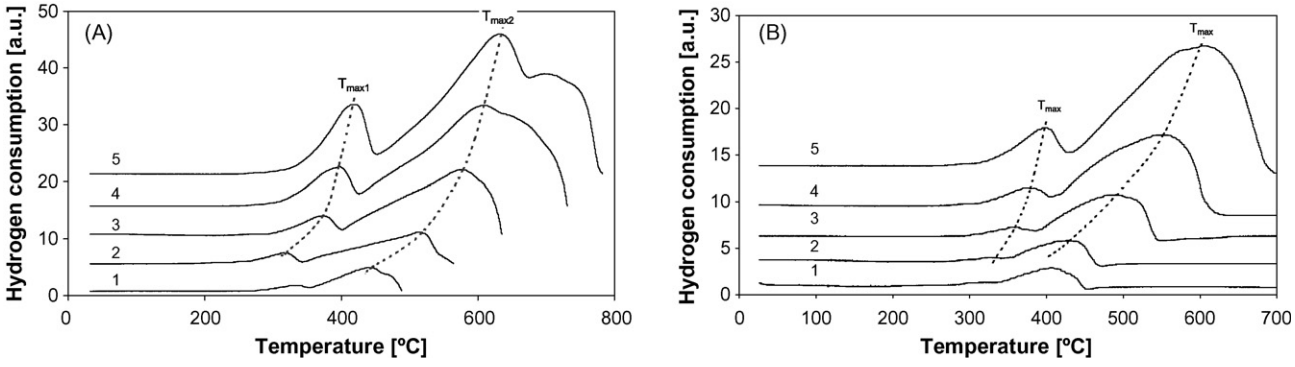

Fig. 1. Influence of heating rate on TPR_{H2} profiles for α-Fe_2O_3: (A) 50 mg; (B) 15 mg; curves: (1) 0.58; (2) 1.07; (3) 2.57; (4) 5.52; (5) 10.7 °C/min.

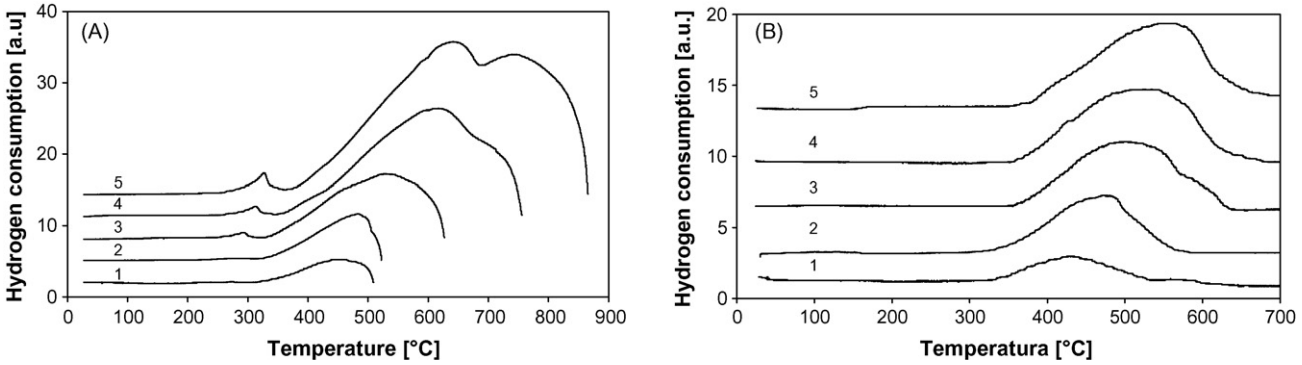

Fig. 2. Influence of heating rate on TPR_{H2} profiles for: Fe_3O_4 (A) and FeO (B); curves: (1) 0.58; (2) 1.07; (3) 2.57; (4) 5.52; (5) 10.7 °C/min.

difficult to recognize as a distinct peak for very low heating rate but the assignment of this TPR peak seems to be beyond any doubts, $Fe_2O_3 \rightarrow Fe_3O_4$ and the acknowledgment of the second TPR peak can be much more sophisticated than merely direct reduction of magnetite to metallic iron, $Fe_3O_4 \rightarrow Fe$. One can anticipate the two-step reduction, magnetite $Fe_3O_4 \rightarrow$ wüstite $Fe_{1-x}O \rightarrow$ iron Fe^0, occurring when temperature of reduction is higher than 570 °C, when wüstite is thermodynamically stable. Such two-step magnetite reduction behavior can be anticipated for rapidly heated samples when diffusion limitations of reduction play an essential role as rate determining factors.

TPR_{H2} profiles of commercial iron oxides, magnetite and wüstite are presented in Fig. 2A and B, respectively.

In the case of magnetite, the similarity to hematite reduction is obvious (compare Fig. 1) but the small residual reduction peak located at about 300 °C is assigned to the hematite type impurity already present in the original sample of magnetite but not recognizable as appropriate XRD pattern (compare curves 3 and 4 in Fig. 6). The reduction of wüstite takes place in the same temperature region as magnetite does, above 320 °C. The most characteristic feature of wüstite reduction profile is the more symmetrical shape of the reduction peak in comparison to the TPR_{H2} peaks characterizing magnetite and hematite reduction processes, but evident nonsymmetrical tailing on both sides of FeO reduction peak can be observed. In fact, the same temperature range of magnetite and wüstite reductions may suggest their related reduction mechanistic pathways instead of a frequently postulated two-step reduction sequence, $Fe_3O_4 \rightarrow FeO \rightarrow Fe$.

On the basis of TPR_{H2} profiles, given in Figs. 1 and 2, the calculated temperature-programmed ''Arhenius plots'' are straight lines for: hematite, magnetite and wüstite [45], and they are shown in Fig. 3.

The activation energy can be determined independently of the reduction mechanism applying the position of the TPR peak maximum at different heating rates. And the activation energies of reduction calculated with slope – E/R were 70 and 52 kJ/mol, respectively for hematite two-step reduction $Fe_2O_3 \rightarrow Fe_3O_4$ and $Fe_3O_4 \rightarrow Fe$; 55 kJ/mol for magnetite reduction $Fe_3O_4 \rightarrow Fe$ and 104 kJ/mol for wüstite reduction $FeO \rightarrow Fe$ and the evaluated values are rather comparable to those found in literature [13–15]. The very close obtained values for magnetite reduction and for the second step of hematite reduction seems to confirm the same mechanism of reduction in both cases. The nearly twice higher value of the activation energy of wüstite reduction suggests a considerably different and strongly temperature dependent mechanism.

The comparison of hydrogen reduction behavior of five iron oxidic compounds—two oxy-hydroxides, goethite α-$FeOOH{\cdot}xH_2O$ and ferrihydrite $Fe_5HO_8{\cdot}4H_2O$, and three iron oxides, hematite α-Fe_2O_3, magnetite Fe_3O_4 and wüstite FeO—are illustrated in Fig. 4 as TPR_{H2} profiles with a heating rate of 1.07 °C per min and nearly the same mass of sample, about 15 mg.

The mutual differences between TPR profiles reflect both the chemical composition of samples and their bulk and surface properties acquired during sample preparation. In the case of the reduction of ferrihydrite, one can notice rather broad monotonic uptake of hydrogen, above 150 °C. For goethite the accompanying desorption effect located in temperature range 150–250 °C is assigned to the decomposition of nitrate ions which were not washed out entirely during the sample precipitation. The evolution of nitrogen oxides was independently confirmed by the MS method. Despite the expected differences in morphology and the degree of hydration, the TPR_{H2} profiles of iron(III) oxides and oxy-hydroxides are generally similar.

The results of BET specific surface area for the above iron oxidic compounds are presented in Table 2.

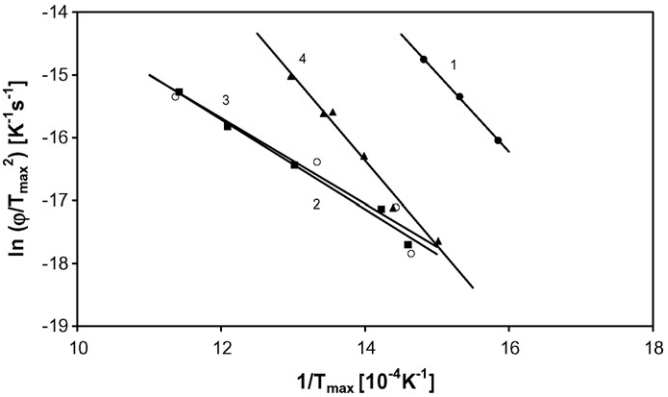

Fig. 3. Arhenius plot of TPR_{H2} profiles for: hematite (1, 2); magnetite (3) and wüstite (4). (1) E_a = 70 kJ/mol for $Fe_2O_3 \rightarrow Fe_3O_4$; (2) E_a = 52 kJ/mol for $Fe_3O_4 \rightarrow Fe$; (3) E_a = 55 kJ/mol for $Fe_3O_4 \rightarrow Fe$; (4) E_a = 104 kJ/mol for $FeO \rightarrow Fe$.

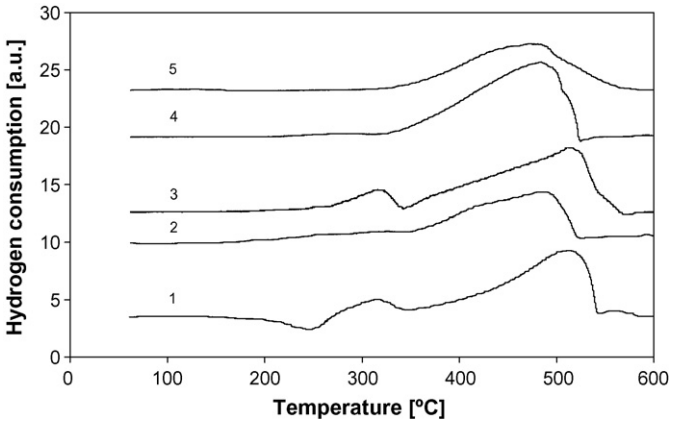

Fig. 4. TPR_{H2} profiles for: (1) goethite; (2) ferrihydrite; (3) hematite; (4) magnetite; (5) wüstite; heating rate 1.07 °C/min.

The samples of oxy-hydroxides dried at 60 °C show relatively high surface area (20–35 m^2/g) in accordance with the entirely amorphous structure of ferrihydrite and rather low crystallinity of goethite structure. The hematite sample calcined at 600 °C shows comparable surface area to those characteristic of oxy-hydroxides, but commercial samples magnetite and wüstite show only about 6 m^2/g and below 1 m^2/g, respectively. The particle size of about 0.22 μm for magnetite and 1.3 μm for wüstite can be estimated assuming spherical and nonporous particles. In fact, a highly dispersed system of wüstite with the crystallites of about 130 nm can be anticipated on the basis of XRD measurements. Thus, instead of a uniform system consisting of the individual and rather similar particles, the different-sized agglomerates of crystallites can be expected.

In order to get a deeper insight into both the reduction and the accompanying dehydration, the additional TG-DTA measurements were carried out. The obtained DTG curves representing the effects of thermal treatment of iron oxidic compounds, in pure hydrogen stream with a linear heating rate 5 °C per min, are presented in Fig. 5.

In the case of oxy-hydroxides, α-$FeOOH{\cdot}xH_2O$ and $Fe_5HO_8{\cdot}4H_2O$, their two-step dehydration occur below 300 °C. The second step of ferrihydrite dehydration is heavily overlapped with the first reduction step occurring in the temperature range 150–350 °C (compare also curve 2 in Fig. 4). One can see that the first stage of ferrihydrite and goethite reduction is not strongly influenced by the excessive desorption of water, originating from adsorbed and structural water. After the preparation procedure, these samples were dried only at 60 °C. The entire reduction of all samples is accomplished to about 550 °C. One can notice a symmetrical shape of DTG peak of wüstite reduction in comparison with the rather asymmetrical peaks representing the reduction of remaining samples. The second and dominant reduction effects located in the temperature range 350–550 °C are analogous for all samples of iron oxides and oxy-hydroxides.

Table 2
The results of BET specific surface area for iron oxidic compounds

Iron oxide	Air pretreatment $T_{calc.}$ (°C)	Surface area (m^2/g)
Goethite	60	34.5
Ferrihydrite	60	21.9
Hematite	600	23.5
Magnetite	Commercial	5.6
Wüstite	Commercial	1.0

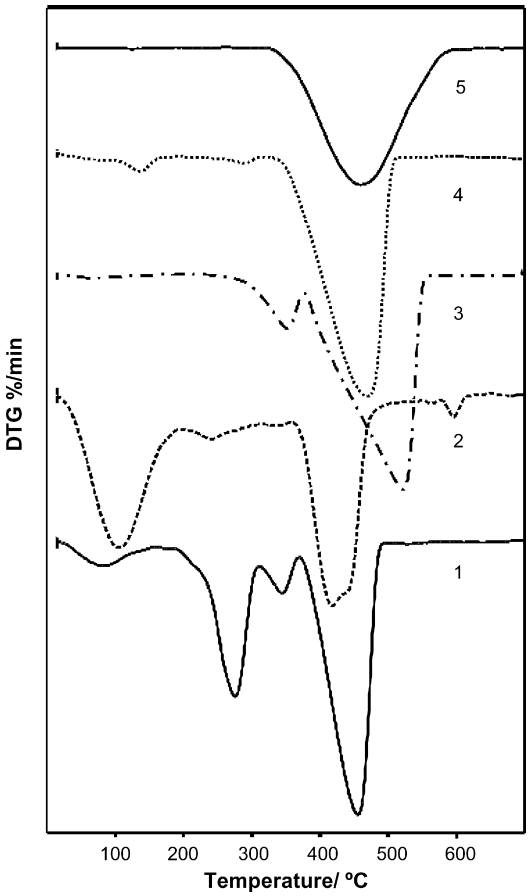

Fig. 5. DTG curves of reduction in pure hydrogen for: (1) goethite; (2) ferrihydrite; (3) hematite; (4) magnetite; (5) wüstite.

The XRD patterns of fresh powdered samples of the investigated five oxidic iron compounds are presented as curves 1–5, respectively, in Fig. 6 and only the sample of ferrihydrite shows fully amorphous structure.

The "*in situ*" XRD powder diffraction patterns obtained in the course of α-Fe_2O_3 reduction in hydrogen atmosphere of 5% H_2–95% Ar gas stream are illustrated in Fig. 7, whereas the calculated changes of phase composition in function of reduction temperature are presented in Fig. 8.

In temperature range from 150 to about 400 °C the first step of hematite to magnetite reduction, $3Fe_2O_3 \rightarrow 2Fe_3O_4$, takes place. At 400 °C, the maximal content of magnetite, about 97%, reflects almost the entire disappearance of hematite phase and the very beginning of metallic iron formation. In temperature range of 400–560 °C the second step, that is reduction of magnetite to metallic iron, occurs, $Fe_3O_4 \rightarrow 3$ α-Fe, and the resulting gradual decrease in magnetite content is observed in favor of the enhancement of metallic iron formation. At 580 °C, the additional wüstite phase appears and three phases are observed: Fe_3O_4 (53%), FeO (7%) and Fe (40%). Thus, the

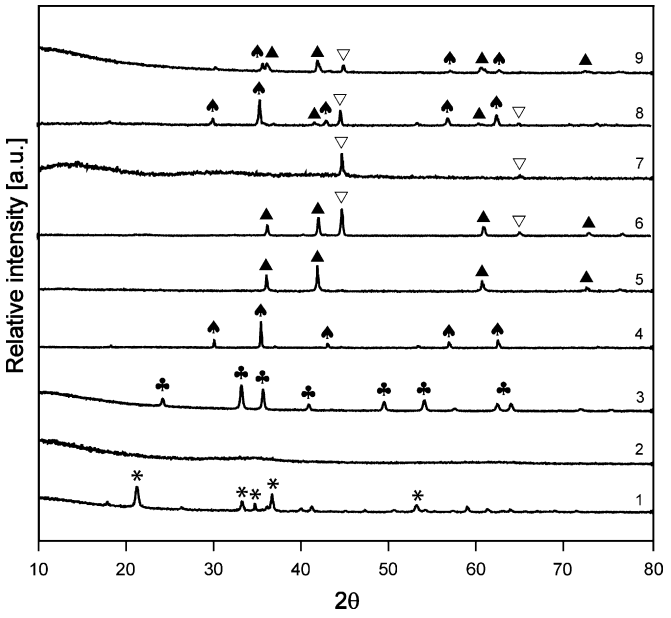

Fig. 6. XRD patterns for: (1) α-FeOOH; (2) $Fe_5HO_8{\cdot}4H_2O$; (3) α-Fe_2O_3; (4) Fe_3O_4; (5) FeO; (6) α-Fe_2O_3 (after TPR_{H2} up to 650 °C); (7) α-Fe_2O_3 (after 4 h in pure CO at 500 °C); (8) FeO (after 10 h in Ar at 500 °C); (9) FeO (after TPR_{CO} up to 600 °C), where: (*) getite; (♣) hematite; (♠) magnetite; (▲) wüstite; (▽) iron.

appearance of wüstite phase proves the involvement of a third step in the reduction of hematite, and the simultaneous occurrence of those three phases also confirms a two-step magnetite reduction pathway, $Fe_3O_4 \rightarrow FeO \rightarrow Fe$. The next stage at 600 °C results in the disappearance of Fe_3O_4 phase and leads back to two-phase system FeO (41%) and Fe (59%). In the applied conditions of the experiment the reduction of wüstite to metallic iron, $FeO \rightarrow Fe$ is entirely accomplished at 680 °C.

The same temperature range of both magnetite and wüstite reduction processes (see Fig. 2A and B) and their mutual similarities in TPR_{H2} behavior seem to be rather contradictive signs for the expected gradual sequence of reduction $Fe_3O_4 \rightarrow FeO \rightarrow Fe$. One can anticipate the involvement of disproportionation reaction $4FeO \rightleftharpoons Fe_3O_4 + Fe$ during wüstite or wüstite like intermediate in the course of magnetite (hematite) reduction. The disproportionation of FeO reflects the formation of both metallic iron phase ($Fe^{2+} \rightarrow Fe^0$) and a stoichiometrical amount of magnetite phase ($3Fe^{2+} \rightarrow 2Fe^{3+} + Fe^{2+}$). The "*in*

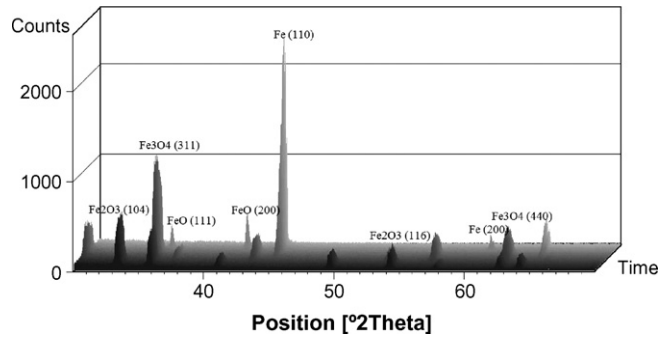

Fig. 7. The "*in situ*" XRD patterns for hematite during temperature programmed reduction in 5%H_2–95% Ar.

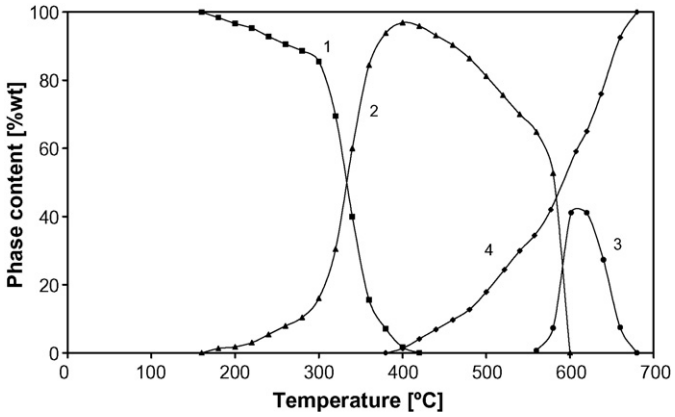

Fig. 8. Phase composition during "*in situ*" XRD temperature programmed reduction of hematite in 5% H_2–95% Ar stream: (1) Fe_2O_3; (2) Fe_3O_4; (3) FeO; (4) Fe.

situ" XRD powder diffraction patterns obtained in the course of temperature programmed reduction of commercial FeO in hydrogen atmosphere of 5% H_2–95% Ar gas stream are presented in Fig. 9, whereas the calculated changes of phase composition in function of reduction temperature are given in Fig. 10.

In temperature range of 150–400 °C, the simultaneous appearance of Fe_3O_4 and Fe phases combined with an appropriate diminishment of FeO phase content and at the same time the lack of wüstite reduction effects prove the occurrence of redox disproportionation of wüstite, not involving hydrogen consumption (compare Figs. 2B, 8 and 9). The mutual changes of molar ratios are close to stoichiometric relations for this reaction. Thus, at still higher temperatures, above 400 °C, the uptake of hydrogen can be engaged both in the reduction of wüstite disproportionation product, that is magnetite, and/or in the reduction of the

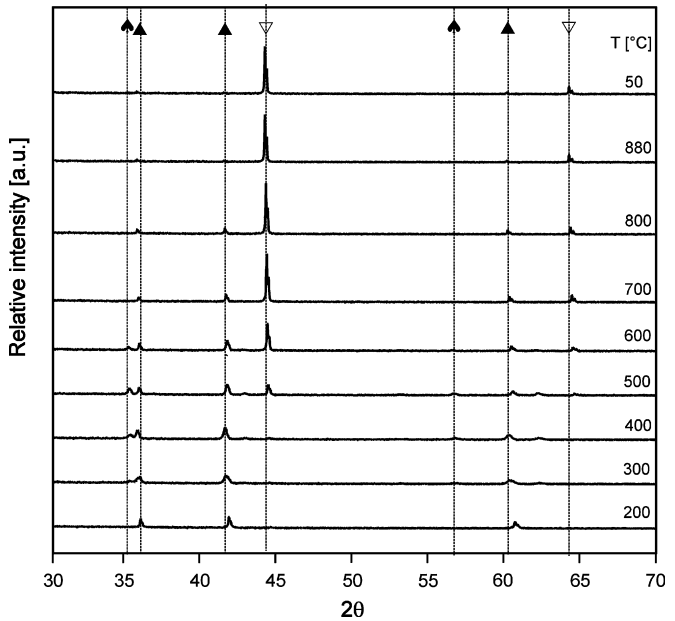

Fig. 9. The "*in situ*" XRD patterns for wűstite during temperature programmed reduction in 5%H_2–95% Ar atmosphere, where: (▽) Fe; (▲) FeO; (♠) Fe_3O_4.

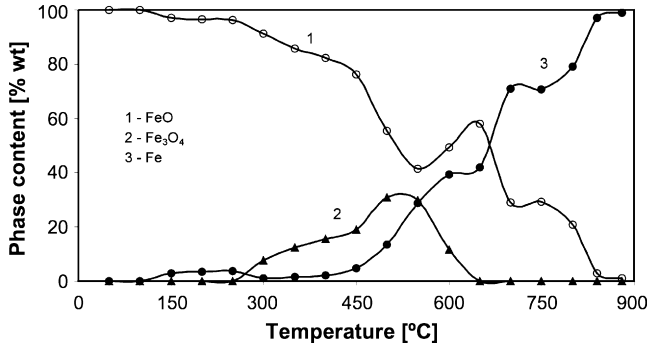

Fig. 10. Phase composition during temperature programmed reduction of wűstite in 5% H_2–95% Ar atmosphere: (1) FeO; (2) Fe_3O_4; (3) Fe.

remaining wüstite phase. The content of magnetite phase reaches maximum value, slightly above 500 °C, and goes down to final disappearance at about 600 °C, and this effect is accompanied by local increase in wüstite content. In the temperature range of 550–700 °C the reverse reaction of wüstite disproportionation can be anticipated. Up to 850 °C the entire reduction of FeO is accomplished. Thus, depending on temperature, instead of one-step simple reduction FeO → Fe, the much more complex two-step pathway FeO → Fe_3O_4 → Fe up to 570 °C or even the three-step complete sequence FeO → Fe_3O_4 → FeO → Fe in the range from 150 to 850 °C should be reconsidered as a result of the accompanying wüstite disproportionation 4 FeO ⇌ Fe_3O_4 + Fe manifesting the primary role above 150 °C and the reversal role from 550 to 700 °C. In the course of FeO reduction in hydrogen atmosphere the non-stoichiometric wüstite like $Fe_{1-x}O$ or magnetite like $Fe^{II}_{1-x}Fe^{III}_{2+x}O_{4+x/2}$ iron oxides were detected, for example $Fe_{0.920}O$, $Fe_{0.880}O$ and $Fe_{2.926}O_4$. During the "in situ" XRD wüstite reduction the particle size of the involved phases undergoes considerable changes in function of the temperature of FeO reduction. The calculated size of metallic iron particles increases monotonically from about 3 nm at 200 °C to about 37 nm at 880 °C. The initial size of wüstite particles was about 130 nm and decreased to about 50 nm at 300 °C, and then a continuous enhancement of particle size was observed to be about 200 nm at 800 °C. The estimated particle size of Fe_3O_4 phase was 20–50 nm in the temperature range 300–600 °C. The characteristic feature is the comparable sizes of FeO and Fe_3O_4 particles.

The transformation of wüstite into magnetite and metallic iron in inert atmosphere of argon (10 h at 500 °C) was also experimentally confirmed and an appropriate XRD pattern is presented as curve 8 in Fig. 6. The influence of treatment temperature on "*in situ*" XRD powder diffraction patterns obtained in the course of the heating treatment of wüstite in neutral atmosphere of argon is illustrated in Fig. 11.

The metallic iron and magnetite phases can be identified in the temperature range 200–680 °C. The additional intermediate XRD reflections and the observed shifts of 2Θ value locations were attributed to the disordered crystal structure deformation forced by both wüstite disproportionation process and natural tendency of wüstite $Fe_{1-x}O$ and magnetite $Fe^{II}_{1-x}Fe^{III}_{2+x}O_{4+x/2}$ changes to their non-stoichiometrical state (Table 1). The

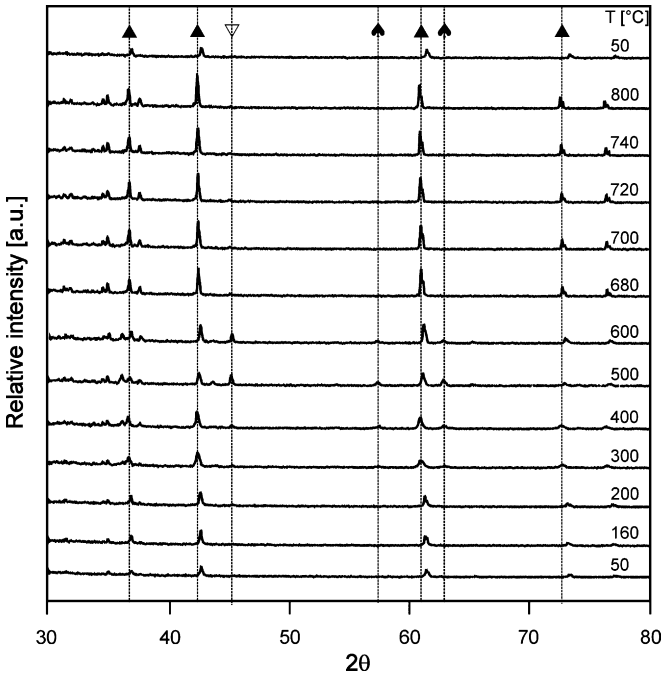

Fig. 11. The "*in situ*" XRD patterns for wüstite during temperature programmed treatment in Ar atmosphere, where: (▽) Fe, (▲) FeO, (♠) Fe_3O_4.

temperature cycle 50 °C → 800 °C → 50 °C in argon atmosphere seems to confirm the fully reversible character of wüstite disproportionation reaction 4 FeO ⇌ Fe_3O_4 + Fe.

3.2. Carbon monoxide reduction

The TPR_{CO} profiles representing iron oxidic compounds goethite, ferrihydrite, hematite, magnetite and wüstite, obtained with heating rate 1.07 °C per min in 5% CO–95% Ar gas stream are illustrated in Fig. 12.

Temperature programmed reduction profiles reflecting CO consumption were the exact mirror images of evolved CO_2, up to 500 °C, and the ion concentration curves (m/z = 44) are presented in Fig. 12. For goethite, ferrihydrite and hematite samples, the reduction effects located in temperature range 150–300 °C are assigned to the first reduction step. The easier reducibility is observed for the hydroxylated samples of

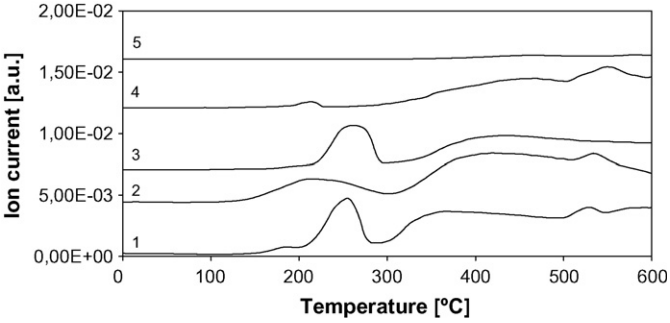

Fig. 12. Carbon dioxide evolution profiles during TPR_{CO} in 5% CO–95% Ar atmosphere for (1) goethite; (2) ferrihydrite; (3) hematite; (4) magnetite; (5) wüstite.

ferrihydrite and goethite. Above 300 °C, the second reduction step representing a further reduction takes place. Above 500 °C, the additional evolution of CO_2 was also accompanied by CO desorption and both the peaks were attributed to surface desorption effects for goethite, ferrihydrite and magnetite samples. In the case of wüstite, a considerably smaller CO reducibility was found and it is confirmed by the TPR_{CO} profile in Fig. 12. The reduced FeO sample after reaching 620 °C was quenched and finally, the XRD pattern was taken after contact of sample with air at ambient temperature (curve 9 in Fig. 6). As expected, the main unreduced wüstite phase was accompanied by metallic iron as the major reduction product. However, the significant presence of magnetite phase was attributed to wüstite disproportionation reaction $4FeO \rightarrow Fe_3O_4 + Fe$ taking place also in reductive atmosphere 5% CO–95% Ar during TPR_{CO} run, up to 620 °C. The traces of iron carbide phase Fe_xC were also detected.

In order to get deeper insight into CO reduction of hematite, the analogical TG–DTA–MS measurements were performed in 5%CO–95% Ar gas stream, and they are presented in Fig. 13 as TG, DTG and DTA curves and MS profiles of ion concentration for CO ($m/z = 28$) and CO_2 ($m/z = 44$), respectively.

Three-step CO reduction of hematite takes place in the temperature range 200–600 °C and this process is additionally accompanied by the highly exothermic process of the formation of carbon deposit on the surface of reduced sample, attributed to carbon monoxide disproportionation reaction $2CO \rightarrow C + CO_2$ occurring above 400 °C. Carbon deposition seems to be auto-catalyzed by metallic iron produced in final step of hematite reduction and its efficiency is strongly influenced by the concentration of carbon monoxide gas and the heating rate of sample [28]. The amorphous graphite like deposit and metallic iron phases, were identified by the conventional XRD method as the final products of hematite reduction, 4 h at 500 °C in pure CO (see curve 7 in Fig. 6). Also, depending on the conditions of carbon diffusion into metallic network (temperature, time) iron carbides Fe_xC can be formed, especially when reduction temperature is higher than 600 °C.

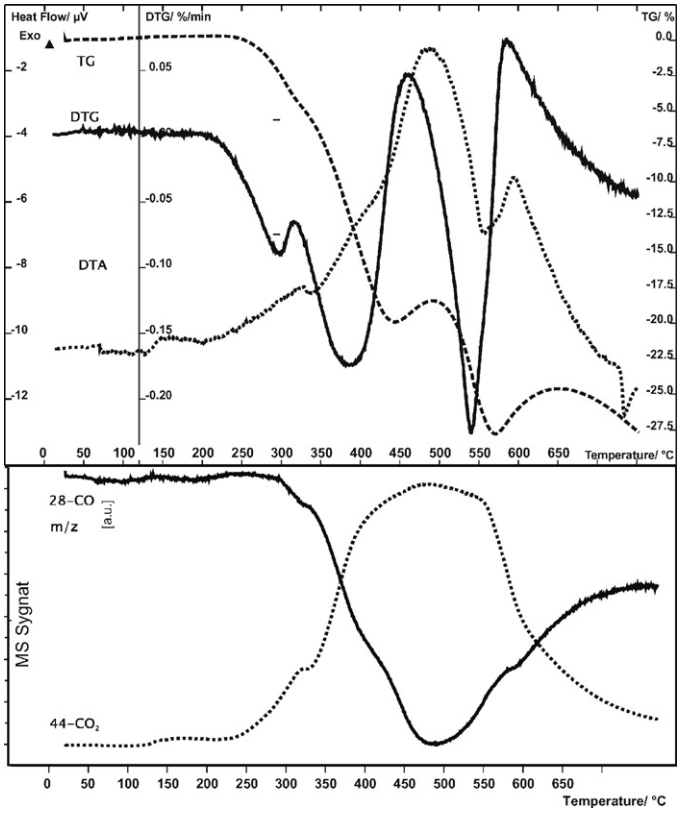

Fig. 13. TG–DTA–MS curves for TPR_{CO} hematite reduction.

4. Discussion

At temperatures below 570 °C, the absence of wüstite phase as an intermediate of both hematite and magnetite reduction in hydrogen is not an experimental prerequisite condition during an atomic scale reduction $Fe^{3+} \rightarrow Fe^{2+} \rightarrow Fe^0$ taking place on an interface border between formed metallic iron and reduced magnetite phases Fe/Fe_3O_4 [13,14]. During reduction each hydrogen molecule reacts with an interface oxygen atom O_s giving water molecule and anionic vacancy:

$$O_s + H_2 \rightarrow \square + H_2O \quad (1)$$

A source of electron responsible for reduction step $Fe^{3+} \rightarrow Fe^{2+}$ could be an interface oxygen vacancy located on Fe^{2+} according to an equation representing water desorption step as the result of two hydroxyl group condensation [13,14]:

$$2\,Fe^{3+} - OH \rightarrow Fe^{3+} - O + Fe^{2+} + H_2O \quad (2)$$

The above reaction plays significant role not only in the initial dehydration–dehydroxylation processes taking place at the beginning of iron oxy-hydroxides (ferrihydrite and goethite) reduction but it would also be crucial in every reduction stage of iron oxides (hematite, magnetite and wüstite). Usually, in the initial stage of iron oxide reduction, the chemisorptive dissociation of hydrogen molecule is involved resulting in the intermediate hydroxyl group formation according to general scheme: $2\ O^{2-} + H_2 \rightarrow 2\,OH^- \rightarrow O^{2-} + H_2O$. Thus, the removal of individual water molecule could serve as a unit measure of iron oxide reduction degree. The same role can be assigned to cationic ratios Fe^{2+}/Fe^{3+} and/or Fe^0/Fe^{2+}. The two-step hematite reduction can be represented by the two following equations:

$$3\alpha\text{-}Fe_2O_3 + H_2 \rightarrow 2\,Fe_3O_4 + H_2O \quad (3)$$

$$2\,(Fe_3O_4 + 4\,H_2 \rightarrow 3\,Fe + 4\,H_2O) \quad (4)$$

Formally, the last process of magnetite reduction directly to metallic iron (equation (4)) can be described by a sum of two subsequent steps:

$$2\,(Fe_3O_4 + H_2 \rightarrow 3\,FeO + H_2O) \quad (5)$$

$$6\,(FeO + H_2 \rightarrow Fe + H_2O) \quad (6)$$

Finally, a sequence of equations (3) and (4) is responsible for the two-step hematite reduction, whereas a sequence of equations (3), (5) and (6) represents the three-step hematite reduction. In equations (3)–(6), the same mode of one

hydrogen molecule consumption was applied as equivalent of one oxygen atom removal in general equation (1). Taking into account the atomic scale of hematite reduction both reactions (5) and (6) would occur whether or not wüstite phase is formed. From kinetics point of view slow reaction (5) and fast reaction (6) would be responsible for the presence of Fe_3O_4 and the absence of FeO intermediates in low temperature range of hematite reduction. Above 570 °C, the reverse takes place—fast reaction (5) and slow reaction (6) are responsible for the absence of Fe_3O_4 and the appearance of FeO intermediates.

In low temperature range wüstite is unstable phase and above 150 °C it is partially transformed into Fe_3O_4 and Fe phases as a result of disproportionation reaction not consuming hydrogen:

$$4\,FeO \rightleftharpoons Fe_3O_4 + Fe \qquad \Delta G^0 = -6.9\,kJ\,mol^{-1} \tag{7}$$

The high temperature treatment of wüstite up to 780 °C in inert atmosphere confirms the reversible character of temperature activated process of disproportionation. The reduction of wüstite to metallic iron in hydrogen or carbon monoxide is not a simple one-step process because it is accompanied by disproportionation reaction regardless of the fact of reductive atmosphere. At low temperature, above 150 °C, the disproportionation reaction takes place whereas in most cases reduction of magnetite starts above 350 °C. In such situation instead of one-step simple reduction $FeO \rightarrow Fe$, a much more complex two-step process $FeO \rightarrow Fe_3O_4 \rightarrow Fe$ up to 570 °C or even a three-step reduction $FeO \rightarrow Fe_3O_4 \rightarrow FeO \rightarrow Fe$ will operate up to 850 °C.

The presence of water and its partial pressure in hydrogen stream H_2O/H_2 play a crucial role not only affecting the kinetics of water desorption and its diffusion but also influencing the thermodynamics of the system $Fe_2O_3/Fe_3O_4/Fe_xO/Fe$. Both the retardation of reduction $Fe_3O_4 \rightarrow Fe$ and the acceleration of H_2 dissociation by metallic Fe and the subsequent hydrogen spillover by H_2O can influence the reduction kinetics in negative and/or positive way, respectively [13,16,29].

Below 570 °C, the experimentally evidenced presence of thermodynamically unstable wüstite as an intermediate of the reduction of an unsupported iron(III) oxidic compounds is rather seldom in literature. The low temperature formation of wüstite, below 500 °C was observed during the reduction of magnetite and hematite [30,31]. The presence of wüstite in the oxidized form of iron catalysts for ammonia synthesis (doped with Al_2O_3, SiO_2, CaO and K_2O) is rather common [32–34]. Frequently, wüstite appears in bi-oxide systems or iron supported catalysts. The stabilization of metastable wüstite phase on oxidic support surface (MgO, SiO_2, Al_2O_3) is considered as an indication of strong FeO—support interphase interactions or solid solutions and/or appropriate chemical compounds [10,26,28,35–43]. Often, the low loaded samples of iron oxide/support catalysts hardly ever revealed the presence of metallic iron phase after high temperature reduction of catalyst in hydrogen or carbon monoxide atmospheres.

According to Spitzer et al. [5] when the sample is reduced at a temperature above 700 °C in the usual topochemical way oxygen weight loss occurs at three reaction interfaces Fe/Fe_xO, Fe_xO/Fe_3O_4 and Fe_3O_4/Fe_2O_3. The mechanism of iron-oxide reduction leads to a rather the unavoidable conclusion that the nature of the total process is extremely complex and may vary with the physico-chemical characteristics of oxide specimen or with the conditions of reduction.

The hydrogen reduction behavior of Fe_2O_3, Fe_3O_4 and FeO is strongly influenced by the temperature–time–pressure dependent process. According to some literature sources, the only intermediate is magnetite, whereas others postulate both magnetite and wüstite. As FeO is thermodynamically unstable below 576 °C [44], any reduction beyond Fe_3O_4 should give Fe metal and this is the case in the presented paper [19]. Only when the Fe_2O_3 phase disappears the reduction of Fe_3O_4 to Fe can be observed. The present data show that during the first stage of hematite reduction one-third of Fe^{3+} ions are reduced to Fe^{2+} ions. Our experimental data prove the existence of FeO phase above 570 °C as an intermediate in the course of Fe_3O_4 reduction regardless of diffusion or kinetic limitations. In temperature range 350–570 °C instead of direct magnetite reduction to iron, $Fe_3O_4 \rightarrow Fe$, the two-step process is still possible, at least in atomic scale on the surface of magnetite. Assuming the reversible character of FeO disproportionation $4\ FeO \rightleftharpoons Fe_3O_4 + Fe$, the coexistence of both reaction products, Fe_3O_4 and Fe in direct contact, which is the case of magnetite reduction in hydrogen, should result at least in FeO surface species located in the interface region between Fe_3O_4 and Fe. The formation of ordered FeO (1 1 1) domains as intermediate reduction species on Fe_3O_4 surface was reported [44]. The disproportionation reaction: wüstite ⇌ magnetite + iron makes simple wüstite reduction $FeO \rightarrow Fe$ a more complicated process. In the case of thermodynamically forced FeO disproportionation the cubic sub-lattice of oxygen atom network does not change during wüstite → magnetite transformation and only the process of metallic iron phase formation requires temperature activated diffusion of iron atoms into the inter-phase FeO/Fe_3O_4 region.

5. Conclusions

The approach of the temperature dependent reduction mechanism is common for all iron oxides (Fe_2O_3, Fe_3O_4, FeO) or iron oxy-hydroxides (FeOOH, $Fe_5HO_8{\cdot}4H_2O$) after a low-temperature dehydration (<300 °C). The key factor the temperature 570 °C is the lowest border limit of the thermodynamic stability of FeO. Below that temperature FeO disproportionation reaction, $4FeO \rightarrow Fe_3O_4 + Fe$ is shifted toward products, whereas above that temperature the reverse reaction $Fe_3O_4 + Fe \rightarrow 4FeO$ dominates. The disproportionation reaction occurs in neutral atmosphere and although it does not involve hydrogen but it can influence the mechanism of the reduction of iron oxides in hydrogen. Depending on the reduction temperature the proposed paths of

iron oxides reduction can be assigned to the following schemes:

Hematite:

$Fe_2O_3 \rightarrow Fe_3O_4 \rightarrow Fe$ (below 570 °C)

$Fe_2O_3 \rightarrow Fe_3O_4 \rightarrow FeO \rightarrow Fe$ (below and above570 °C)

Magnetite:

$Fe_3O_4 \rightarrow Fe$ (below 570 °C)

$Fe_3O_4 \rightarrow FeO \rightarrow Fe$ (below and above 570 °C)

Wüstite:

$FeO \rightarrow Fe_3O_4 \rightarrow Fe$ (below 570 °C)

$FeO \rightarrow Fe_3O_4 \rightarrow FeO \rightarrow Fe$ (below and above 570 °C)

$FeO \rightarrow Fe$ (below and above 570 °C)

The first step of $Fe_2O_3 \rightarrow Fe_3O_4$ reduction requires the transformation of oxygen sub-lattice combined with iron atoms dislocation. The second step of $Fe_3O_4 \rightarrow Fe$ reduction requires the nucleation sites of metallic Fe phase. The third step of $Fe_3O_4 \rightarrow FeO$ reduction does not require any transformation of oxygen sub-lattice. It can take place at higher temperatures than 570 °C. Also, the reverse disproportionation of FeO favors this reaction but an essential role is attributed to an interface in direct contact of magnetite with metallic iron, and such border does exist in the second step of $Fe_3O_4 \rightarrow Fe$ reduction and in this way this reduction step can be replaced by the reverse disproportionation of FeO. The mechanism of $FeO \rightarrow Fe$ reduction is relatively simple but only at temperatures higher than 570 °C. A much complicated process of FeO reduction is in simpler case a sequence of two-step $FeO \rightarrow Fe_3O_4 \rightarrow Fe$ or even, three-step $FeO \rightarrow Fe_3O_4 \rightarrow FeO \rightarrow Fe$ reduction. The first step in both cases refers to FeO disproportionation starting above 150 °C and in this way the additional substrate of a subsequent reduction, Fe_3O_4 is formed and equivalent Fe atoms, serving as nucleation sites of metallic iron phase are created. Thus, two parallel reduction paths are possible: $Fe_3O_4 \rightarrow Fe$ and $FeO \rightarrow Fe$ in low-temperature range and only one-path $FeO \rightarrow Fe$ reduction at high-temperatures but only after the accomplishment of the reverse FeO disproportionation, $Fe_3O_4 + Fe \rightarrow 4FeO$. The much higher energy of the activation of FeO reduction (104 kJ/mol) indirectly indicates much more temperature resistant process in comparison with hematite reduction (70 kJ/mol, 52 kJ/mol) and magnetite reduction (55 kJ/mol).

The thermodynamic instability of FeO rather refers to the state of FeO after the formation an appropriate conditions, usually in high temperature, and its final quenching in low temperature conditions. The stable and highly dispersed FeO phase in Fe/support catalyst can be obtained as a result of the strong chemical surface interaction between FeO and support. The additives can play a crucial role in stabilizing FeO particles in magnetite phase. The appearance of FeO crystal phase as an intermediate compound of iron(III) oxide reduction was experimentally confirmed by XRD method above 570 °C. Depending on hydrogen reduction conditions, the complete reduction of hematite into metallic iron phase can be accomplished even at low temperature up to 380 °C in pure hydrogen. Although the reduction behavior is analogical for all examined iron oxides it is strongly influenced by their particle size, crystallinity and the conditions of the temperature–time–pressure dependent reduction.

Acknowledgements

The financial support for this work by the Polish Scientific Research Council (grant no. 4T09 146 25 and no. PBZ-KBN-116/T09/2004) is gratefully acknowledged.

References

[1] R.M. Cornell, U. Schwertmann, The Iron Oxides, New York, 1996.
[2] H. Provendier, C. Petit, C. Estournes, S. Libs, A. Kiennemann, Appl. Catal. A: Gen. 180 (1999) 163.
[3] J. Hua, K. Wei, Q. Zheng, X. Lin, Appl. Catal. A: Gen. 259 (2004) 121.
[4] D.B. Bukur, X. Lang, J.A. Rossin, W.H. Zimmerman, M.P. Rosynek, E.B. Yeh, Ch. Li, Ind. Eng. Chem. Res. 28 (1989) 1130.
[5] R.H. Spitzer, F.S. Manning, W.O. Philbrook, Trans. Metall. Soc. AIME 236 (1966) 726.
[6] J.H.M. Kock, H.M. Fortuin, J.W. Geus, J. Catal. 96 (1985) 261.
[7] H.E. Kissinger, Anal. Chem. 29 (1957) 1702.
[8] A. Baranski, J.M. Lagan, A. Pattek, A. Reizer, Appl. Catal. 3 (1982) 207.
[9] R. Brown, M.E. Cooper, D.A. Whan, Appl. Catal. 3 (1982) 177.
[10] E.E. Unmuth, L.H. Schwartz, J.B. Butt, J. Catal. 63 (1980) 404.
[11] W.K. Jozwiak, T.P. Maniecki, W. Maniukiewicz, Pol. J. Environ. Stud. 14 (2005) 195.
[12] J. Surman, P. Kustrowski, L. Chmielarz, R. Dziembaj, Przem. Chem. 82 (2003) 783.
[13] G. Munteanu, L. Ilieva, D. Andreeva, Thermochim. Acta 291 (1997) 171.
[14] O.J. Wimmers, P. Arnoldy, J.A. Moulijn, J. Phys. Chem. 90 (1986) 1331.
[15] H.Y. Lin, Y.W. Chen, Ch. Li, Thermochim. Acta 400 (2003) 61.
[16] O. Lebedeva, W.H.M. Sachtler, J. Catal. 191 (2000) 364.
[17] A. Slagtern, H.M. Swaan, U. Olsbye, I.M. Dahl, C. Mirodatos, Catal. Today 46 (1998) 107.
[18] Khader, M. Mahmoud, El-Anadouli, E. Bahgat, El-Nagar, Emad, Ateya, G. Badr, J. Solid State Chem. 93 (2) (1991) 283.
[19] T. Herranz, S. Rojas, F.J. Perez-Alonso, M. Ojeda, P. Terreros, J.L.G. Fierro, Appl. Catal. A: Gen. 308 (2006) 19.
[20] K. Chen, Q. Yan, Appl. Catal. A: Gen. 158 (1997) 215.
[21] A. Venugopal, M.S. Scurrell, Appl. Catal. A: Gen. 258 (2004) 241.
[22] U. Schwertmann, R.M. Cornell, Iron Oxides in the Laboratory, Weinheim, 2000, p. 13.
[23] D.A.M. Monti, A. Baiker, J. Catal. 83 (1983) 323.
[24] P. Malet, A. Caballero, J. Chem. Soc. Faraday Trans. 84 (1988) 2369.
[25] H.M. Rietveld, J. Appl. Crystallogr. 2 (1969) 65.
[26] H. Jung, W.J. Thomson, J. Catal. 128 (1991) 218.
[27] W.K. Jozwiak, A. Basinska, J. Góralski, T.P. Maniecki, D. Kincel, F. Domka, Stud. Surf. Sci. Catal. 130 (2000) 3819.
[28] W.K. Jozwiak, T.P. Maniecki, T. Paryjczak, A. Basinska, R. Fiedorow, Kinet. Catal. 45 (6) (2004) 879.
[29] G. Fröhlich, W.M.H. Sachtler, J. Chem. Soc. Faraday Trans. 94 (9) (1998) 1339.
[30] Z.Y. Zhong, T. Prozorov, I. Felner, A. Gedanken, J. Phys. Chem. B 103 (1999) 947.
[31] C.H. Bartholomew, History of cobalt catalyst design for FTS AIChE Meeting, New Orleans, 2003.
[32] W. Arabczyk, Pol. J. Chem. Technol. 7, 3 (2005) 8.
[33] Z. Lendzion-Bieluń, W. Arabczyk, Appl Catal. A: Gen. 207 (2001) 37.

[34] Z. Lendzion-Bieluń, W. Arabczyk, M. Figurski, Appl. Catal. A: Gen. 227 (2002) 255.
[35] A. Lycourghiotis, D. Vattis, React. Kinet. Catal. Lett. 18 (3–4) (1981) 377.
[36] X.P. Dai, Q. Wu, R.J. Li, Ch.Ch. Yu, Z.P. Hao, J. Phys. Chem. B 110 (2006) 25856.
[37] C. Greffie, M.F. Benedetti, C. Parron, M. Amouric, Geochim. Cosmochim. Acta 60 (9) (1996) 1531.
[38] L. Guczi, Z. Paszti, K. Frey, A. Beck, G. Peto, Cs.S. Daroczy, Topics Catal. 39 (3–4) (2006) 137.
[39] W.K. Jozwiak, E. Kaczmarek, W. Ignaczak, Pol. J. Environ. Stud. 14 (2005) 127.
[40] A. Bainska, T.P. Maniecki, W.K. Jozwiak, React. Kinet. Catal. Lett. 89 (2) (2006) 319.
[41] P.G. Caceres, Appl. Catal. 110 (1994) 185.
[42] F. Domka, M. Łaniecki, Surf. Technol. 7 (1978) 217.
[43] M.L. Cubeiro, H. Morales, M.R. Goldwasser, M.J. Perez-Zurita, F. Gonzalez-Jimenez, React. Kinet. Catal. Lett. 69 (2) (2000) 259.
[44] G. Ketteler, W. Weiss, W. Ranke, R. Schlögl, Phys. Chem., Chem. Phys. 3 (2001) 111.
[45] W.K. Jóźwiak, E. Kaczmarek, W. Ignaczak, Determination of reduction mechanism by tpr data for FeO–H_2 system, Pol. J. Chem., submitted for publication.

Reduction behavior of iron oxides in hydrogen and carbon monoxide atmospheres

Article *in* Applied Catalysis A General · June 2007

DOI: 10.1016/j.apcata.2007.03.021